THE MARK II SECONDARY VERTEX DETECTOR*

John A. Jaros
Stanford Linear Accelerator Center
Stanford University, Stanford, California 94305

Summary

We have added a high precision drift chamber to the Mark II detector at PEP. The design of the device has been optimized for measuring vertex topologies as accurately as possible. This has involved placing wires within 10 cm of the beam line, using a beryllium beam pipe as the inner gas wall of the chamber, and improving the accuracy of the drift-time measurement. The chamber operates reliably and efficiently and records complex hadronic events accurately. Although the currents drawn by the chamber are moderately high in colliding beam operations, events are "clean," with few spurious tracks or hits. The spatial resolution of the chamber is 80 μ; this permits tracks to be extrapolated to the interaction point with 100 μ accuracy.

Introduction

During the past year, we[1] have constructed, installed, and begun data taking with a high precision drift chamber which has been added to the Mark II detector at PEP. The chamber, shown in Fig. 1, is located between the vacuum chamber and main Mark II tracking chamber. Its purpose is to provide an accurate picture of the interaction and decay vertices which are produced in high energy e^+e^- interactions. Decays of hadrons containing the c and b quarks and the τ lepton give rise to events with secondary vertices within 1 mm or so of the interaction point. The secondary vertex detector should allow us to measure the location of these secondary vertices accurately enough to determine particle lifetimes. The device may also be useful in tagging events with charm or bottom hadrons.

The design of the chamber was optimized for vertex detection, but it serves in several other capacities as well. It is used at both the primary and secondary levels in the Mark II trigger.[2] As an adjunct to the main tracking chamber, it improves solid angle coverage and momentum resolution, and of course the reconstruction of K^0_S and Λ decays. We hope, in the future, to use it for pattern recognition in events with dense hadron jets.

This paper discusses the mechanical design of the chamber and the techniques we used to enhance its performance as a vertex detector. In addition, it summarizes our brief experience operating the chamber at PEP. It concludes with a discussion of the chamber's performance.

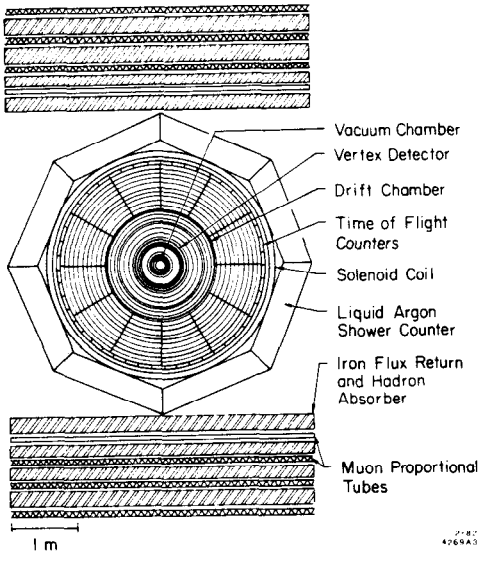

Fig. 1. The Mark II detector at PEP. The muon detection system on the sides is not pictured.

Chamber Parameters

Fig. 2 shows a cross section of the vacuum chamber, the vertex detector, and the innermost wires of the main drift chamber. The vertex detector is a cylindrical drift chamber 1.2 meters long and .70 meters in diameter. Wires are strung between the two 5 cm thick end plates in two "bands," one comprising 4 wire layers just outside the beam pipe, the other 3 wire layers near the outer radius. The chamber uses the vacuum chamber as an inner gas seal. The cylindrical outer shell is made of .18 cm thick aluminum and supports the wire tension load on the end plates. There are 825 sense wires in the entire chamber, 270 in the inner band and 555 in the outer band. Table I gives the radius and number of wires in each of the sense-wire layers. All the sense wires are axial and no attempt is made to measure position along the wires. The drift cell radius is 5.30 mm throughout the entire array. The chamber and beam pipe can be operated at pressures up to 2 atmospheres absolute.

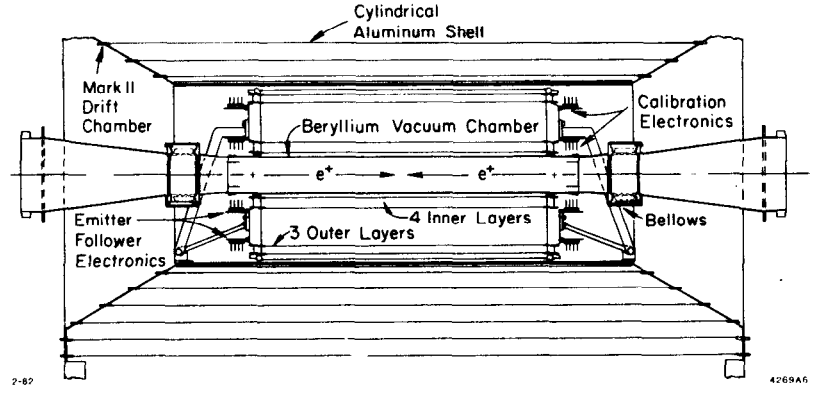

Fig. 2. Cross section of the vertex detector as installed in Mark II.

Table I. Sense Wire Placement in Vertex Detector

	Layer No.	Radius (cm)	No. of Sense Wires
Inner Band	1	10.1223	60
	2	10.9658	65
	3	11.8093	70
	4	12.6528	75
Outer Band	5	30.3668	180
	6	31.2103	185
	7	32.0538	190

Vertex Detector Design

Extrapolated-Track Resolution

The figure of merit of a vertex detector is the accuracy with which a track can be extrapolated to the vicinity of the primary interaction point. In our chamber, there are two important contributions to this "extrapolated-track resolution." The first comes from our finite measurement accuracy, σ_m, and the fact that we must extrapolate the track significantly beyond where it is measured. In the vertex detector, this error can be written

$$\sigma_x = .85\ \sigma_m\ .$$

Multiple coulomb scattering in the beam pipe, chamber gas, and wires gives rise to the other part of the error. The resultant angular uncertainty leads to a position uncertainty once a track has been extrapolated. It can be written

$$\sigma_{MCS} = 95\ \mu/P\ (\text{GeV/c})$$

for this chamber. These two factors, added in quadrature, give the extrapolated track resolution for the device.

We have followed a straightforward strategy to minimize these tracking errors. We have minimized the distance tracks must be extrapolated by placing the inner wire band as close as possible to the beam pipe. We measure the angle of tracks as accurately as possible by placing the outer band of wires at the largest possible radius. And, of course we have tried to achieve good spatial resolution with the drift-time measurement. Multiple scattering has been kept to a minimum by using a small beam pipe radius, letting the beam pipe double as the inner gas wall for the chamber, and using low Z materials in the construction.

Beryllium Beam Pipe

The beam pipe is a 1.40 m long cylinder, 15.6 cm in diameter, made of 1.42 mm thick rolled beryllium sheet.[3] The central beryllium tube has been brazed to an aluminum ring at each end, and this in turn has been electron-beam-welded to an aluminum-stainless steel transition to which the remainder of the beam pipe is welded. The diameter of the tube was chosen to accommodate the swath of synchrotron radiation from the insertion quadrupoles with some clearance. Beryllium was chosen to minimize the thickness of the tube in radiation lengths. A 50 μ thick titanium foil cylinder was inserted inside the beryllium tube and attached with a continuous circumferential weld at each end. Its purpose is to absorb synchrotron radiation which backscatters from heavy masks located 3 meters from the interaction point. We have wrapped the outside of the tube with a 50 μ mylar sheet and 25 μ of aluminum foil; the mylar isolates the beam pipe from the foil, which serves as a ground shield for the chamber. The chamber's gas volume is sealed off with O-rings between the beam pipe and the end-plates of the chamber.

High Resolution Drift Chamber

To achieve high spatial resolution in the vertex detector, we have located the wires with high accuracy, employed high resolution electronics and calibration techniques, stabilized the gas pressure, and operated the chamber at high gain. As seen in Fig. 3, which

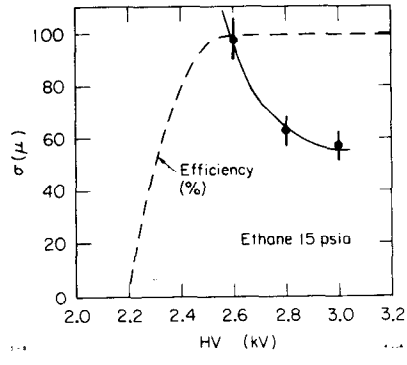

Fig. 3. Spatial resolution as a function of high voltage for pure ethane at 1 atmosphere pressure. The dotted curve shows the efficiency as a function of high voltage. Data are from the vertex detector prototype.

shows spatial resolution in our prototype chamber as a function of chamber voltage, resolution improves significantly when the chamber is operated well above the beginning of the efficiency plateau. The use of organic gases and higher pressure operation should also improve the resolution; once we have assured ourselves that the chamber gas doesn't polymerize in a high background environment, we may try this approach.

Wire Pattern

Fig. 4 shows the wire pattern of the chamber's inner band. The outer band is similar. Two constants characterize the entire array: one is the distance separating a sense wire layer from the adjacent field wire layers (.422 cm); the other is the distance between sense and field wires in a sense-wire layer (.530 cm). With the exception of the outermost and innermost layers, which we call guard layers, all the field wires are run at a common potential; the sense wires are all run at ground potential. Intermediate potentials are chosen for the guard layers to equalize gains on all the sense wires; this also serves to minimize the electrostatic deflections in

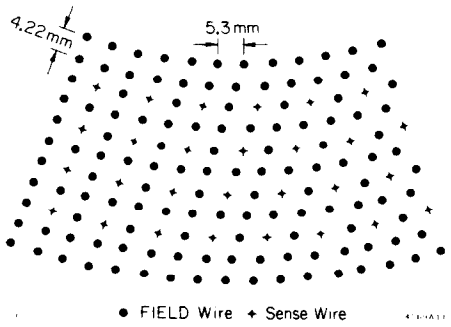

Fig. 4. Arrangement of wires in the vertex detector. The inner band of wires consists of five identical sections; one half section is pictured here.

the array. The presence of a field wire nearly exactly between the two sense wires minimizes cell-to-cell crosstalk. We have used 20 μ diameter gold-coated tungsten wire as sense wires and 150 μ gold-coated field wires. The field wires in the inner band are aluminum, chosen to minimize the multiple coulomb scattering; we use beryllium-copper wire in the outer band. The choice of a fixed sense wire to field wire distance lets us characterize the entire chamber with a single relation between drift time and drift distance. Wires are held in place with the nylon insulating bushing shown in Fig. 5. By selecting the

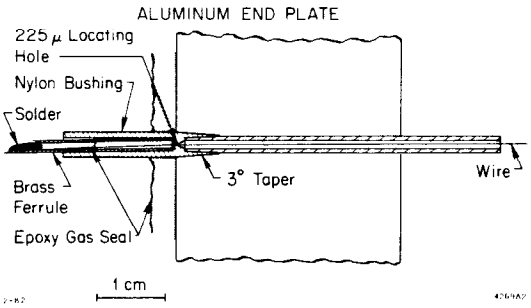

Fig. 5. Nylon insulating and positioning bushing.

bushings individually under a high power microscope and by using high precision machining techniques, we have located the wires to an accuracy of better than 15 μ (rms) throughout the chamber.

Electronics

The electronics associated with the chamber is shown schematically in Fig. 6. Calibration pulses, used to determine a common start time for the entire array, are fanned out to each wire and are simultaneous within 350 ps (rms). The chamber pulse is coupled to 6 m of 50 Ω coax with a fast emitter-follower which serves as an impedance matcher. We use commercial amplifier/discriminators[4] to drive 17 m of twisted pair; the time between a wire pulse and common stop pulse is measured with a time-to-amplitude converter[5] which is readout with a dedicated microprocessor[6] (BADC) which then communicates via camac with the on-line computer. The TAC/BADC resolution is better than 250 ps throughout the entire system. The TAC has additional outputs used in the primary and secondary triggers. During data taking, the system is calibrated every 8 hours.

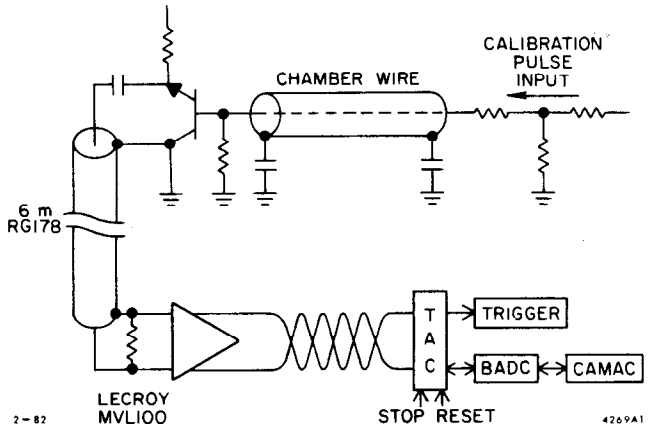

Fig. 6. Calibration and readout electronics.

Operating Experience at PEP

The vertex detector was installed in the Mark II detector at PEP in September of 1981. It was operational for trigger and efficiency studies during the month of November and was used in regular data taking during December when an integrated luminosity of 1500 nb^{-1} was accumulated at 29 GeV center-of-mass energy.

We are operating the chamber at 15.50 ± .05 psia with a 50/50 mixture of argon and ethane. The high voltage is set to 2.250 kV and the electronics threshold is 400 μV at the MVL100 input. With stored currents of 20 ma of both electrons and positrons, there is no beam pickup. Under these same conditions, we have observed a little beam pipe heating; the beam pipe temperature has increased by as much as 3° C when the beams are on. Moderately high currents are drawn by the chamber, especially the inner layers. At the beginning of a fill there is ~ 0.2 μA/wire in the inner band; only 0.01 μA/wire is drawn in the outer band. Despite these rather high currents, the information from the chamber is quite "clean"; i.e., we see very few spurious hits or uncorrelated tracks, and there is no noticeable "snow." Fig. 7 shows the pattern of the wires which have been "hit" in a typical hadronic event in the vertex detector. It also demonstrates that cell-to-cell pickup is not a

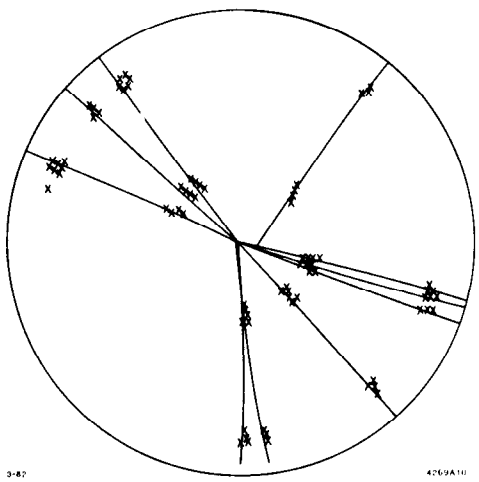

Fig. 7. Hadronic event in the vertex detector.

problem. In general, adjacent cells fire only when a track has passed near enough to a cell boundary that ionization is collected on both wires. Typically, one of the drift-times is very long in these instances.

Chamber Performance at PEP

Efficiency

Fig. 8 shows the chamber efficiency as a function of high voltage for each of the four inner layers.

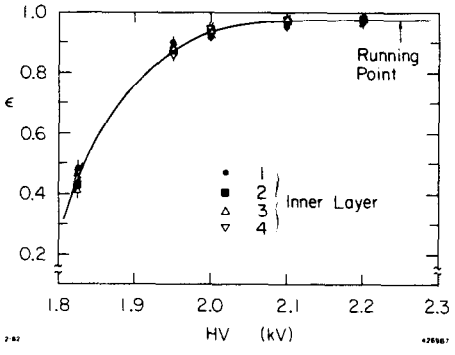

Fig. 8. Efficiency vs. high voltage

Note that, within the statistical errors, all the data seem to lie on one curve. This fact confirms that the wire gains in the four layers have been successfully matched. The chamber is fully efficient above 2050 V; we assume the observed 1 or 2 % inefficiency to be tracking errors, and not a true measure of chamber inefficiency. We run the chamber well above the knee in the efficiency plateau in order to improve the spatial resolution.

Monitoring Drift Velocity

The close packed wire array in the vertex detector is auto-calibrating in the following sense. A typical track passing through the inner layers generates 4 independent drift times. These 4 times can be algebraically related to four other quantities: the slope and intercept of the particle's trajectory, the drift velocity, and the time corresponding to zero drift length. Thus, on a track-by-track basis we can monitor the drift velocity and the stability of the calibration procedure. The linear space-time relation we assume in this procedure is accurate over about 80% of the cell. The technique measures the drift velocity with an error of a few per cent per track; so the drift velocity can be monitored to better than 1/2% in a one or two hour run. We hope to use this technique to study run-to-run drift velocity variations; it will permit corrections to be applied on a short time-scale, if necessary.

Resolution

We are currently studying the time-distance relation and spatial resolution in the vertex detector. Our procedure is to assume a simple form for the relation (we allow linear, quadratic, and cubic terms) and vary the parameters to minimize the ΣX^2 for an ensemble of tracks. Our studies to date have used the sample of Bhabha scatters collected during the month of December.

Fig. 9 shows the distribution of the sum of the squared residuals per track for tracks which have passed through the four inner layers after the time-distance parameters have been optimized. Two track

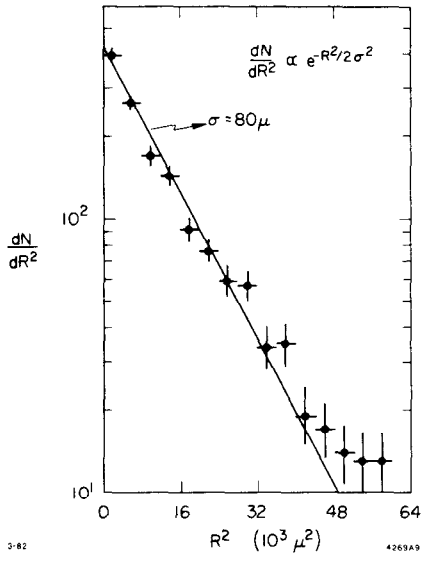

Fig. 9. Distribution of the sum of the squared residuals per track, dN/dR^2.

parameters, the slope and intercept of the trajectory, are allowed to vary in the fit, so the distribution is proportional to the χ^2 distribution for 2 degrees of freedom. So we can write

$$\frac{dN}{dR^2} \propto e^{-R^2/2\sigma^2} \quad ;$$

and the plot lets us determine the resolution graphically. For this subset of the data we have achieved a resolution of 80 μ per layer. We are presently optimizing the time-distance parameters for hadronic events by including angle dependent terms for tracks which pass near the field wires. Assuming a measurement error of 80 μ, the extrapolated track resolution for the Mark secondary vertex detector is

$$\sigma^2 = \sqrt{(70)^2 + \left(\frac{95}{P(\mathrm{GeV/c})}\right)^2} \quad (\mu)$$

Acknowledgements

We acknowledge the help and advice received from many members of the Mark II collaboration. We especially thank M. Breidenbach, L. Golding, V. Golubev, J. Kadyk, T. Nakashima, R. Leonard, and M. Nelson. Thanks also to N. Dean and the PEP Vacuum Group for building, testing, and installing the vacuum chamber.

**Work supported by the Department of Energy, contract DE-AC03-76SF00515.

References

1. D. Amidei, R. Baggs, D. Briggs, E. Grund, G. Hanson, C. Hoard, J. Jaros, D. Johnson, N. Lockyer, R. Stickley, G. Trilling, Y. Wang.

2. H. Brafman et al., IEEE Trans. Nucl. Sci., NS-25 692 (1978).

3. The beryllium chamber was fabricated by Electrofusion Corporation, Menlo Park, CA.

4. LeCroy Research Systems Model 7791 16-channel amplifier/discriminator.

5. E. L. Cisneros et al., IEEE Trans. Nucl. Sci., NS-24 413 (1977).

6. M. Breidenbach et al., IEEE Trans. Nucl. Sci., NS-25 706 (1978).